doi:10.3788/gzxb20124104.0485

Optical Properties of Strained Wurtzite $GaN/Al_{0.15}Ga_{0.85}N$ Cylindrical Quantum Dots: Effects of Hydrostatic Pressure

ZHENG Dong-mei, WANG Zong-chi

(*Department of Physics and Electromechanical Engineering, Sanming College, Sanming, Fujian* 365004, *China*)

Abstract: Within the effective-mass approximation, the influences of hydrostatic pressure on the exciton binding energies, emission wavelengths and electron-hole recombination rates for a heavy-hole exciton in strained wurtzite (WZ) $GaN/Al_{0.15}Ga_{0.85}N$ cylindrical quantum dot (QD) with finite potential barriers are investigated via a variational procedure, with considering the strong built-in electric field (BEF) effect and strain dependence of material parameters. Numerical results show that the exciton binding energies and electron-hole recombination rates both increase almost linearly, and the emission wavelengths are monotonically reduced with the increase of the applied hydrostatic pressure. The hydrostatic pressure has a remarkable influence on the exciton binding energy and electron-hole recombination rate for the QD with a small size. Furthermore, the height of GaN QDs must be less than 5.5 nm for an efficient electron-hole recombination process due to strain effects.

Key words: Quantum dot; Exciton; Hydrostatic pressure; Strain

CLCN: O472^{+}.3 **Document Code**: A **Article ID**: 1004-4213(2012)04-0485-8

0 Introduction

GaN quantum dots (QDs) have attracted considerable attention for some device applications in optics, optoelectronics, and electronics. There have been a number of reports on the fabrication and characterization of various kinds of GaN QDs[1-6]. It was found that a large spontaneous polarization and strain-induced piezoelectric polarization were present in wurtzite (WZ) GaN/AlGaN quantum heterostructures to play an important role in determining the optical and electrical properties via polarization-induced built-in electric fields (BEF), and the magnitude of the BEF was estimated to be in the order of MV/cm[7,8]. Thus, in the past many years, many theoretical works were involved in investigating excitonic states and optical properties of strained $GaN/Al_xGa_{1-x}N$ heterostructures[9-14]. These studies showed that the strong BEF leads to a remarkable reduction of the effective band gap of the heterostructures and gives a significant spatial separation of the electrons and holes in the WZ GaN/AlGaN quantum heterostructures. However, the strain effects in WZ GaN/AlGaN quantum heterostructures should include two parts: 1) the built-in electric field effect; 2) strain dependence of material parameters, such as the effective mass, the effective dielectric constant and the band gap. But the previous studies have not considered the strain dependence of material parameters.

The hydrostatic pressure modifications of the physical properties of nitride based low-dimensional structures are available and helpful for exploring new phenomena and improving devices. Wagner *et al*[15] presented *ab initio* calculations of the structural, dielectric and lattice-dynamical properties of GaN and AlN under hydrostatic pressure. Goñi *et al*[16] investigated experimentally the pressure modification of the phonon modes in wurtzite and zinc-blende GaN and wurtzite AlN. Łepkowski *et al*[17] studied the influence of hydrostatic pressure on the light emission from a strained GaN/AlGaN multiquantum-well system. It was found that the coefficient describing pressure dependence of the peak photoluminescence energy was reduced with respect to the pressure dependence of the energy gap; this could be explainned by the hydrostatic pressure-induced increase of the piezoelectric field in the quantum structures. Ha *et al*[18] explored the influence of screening and hydrostatic pressure

Foundation item: The National Natural Science Foundation of China (No. 11102100)

First author: ZHENG Dong-mei (1971—), female, associate professor, Master, mainly focuses on the theoretical study of the properties of the wide-band gap semiconductor material. Email: smdmzheng@sina.com

Received date: 2011-10-18 **Revised date**: 2011-12-20

on the binding energies of heavy-hole excitons in a strained wurtzite GaN/ $Al_{0.3}Ga_{0.7}N$ quantum well. More recently, Liu *et al*[19] presented the optical property of zinc blend structure GaN under high pressure and obtained two important conclusions: 1) the indirect band gap and the direct band gap widened with pressure increasing; 2) GaN changed from direct band gap to indirect band gap semiconductor when ambient pressure reaches 125 GPa. To the knowledge of authors, the theoretical and experimental works on the exciton states influenced by hydrostatic pressure in a strained wurtzite GaN/$Al_xGa_{1-x}N$ cylindrical quantum dot are still lacking at present. In this paper, we will calculate variationally the exciton binding energy, emission wavelength and electron-hole recombination rate as functions of the QD height and the hydrostatic pressure in a wurtzite GaN/ $Al_{0.15}Ga_{0.85}N$ cylindrical quantum dot with finite potential barriers, considering the strong BEF effect and strain dependence of material parameters.

This paper is organized as follows. In Section 1, a theoretical model used to describe the heavy-hole exciton states confined in the WZ GaN/$Al_xGa_{1-x}N$ cylinderical QD is outlined first, followed by a discussion of the pressure and strain dependence of the material parameters (band gap, effective mass, static dielectric constant *etc*). Numerical results for the exciton binding energy, the interband emission wavelength and the electron-hole recombination rate are given and discussed in Section 2. Finally, we summarize the main conclusions obtained in this paper in Section 3.

1 Theoretical model

1.1 Exciton states in strained wurtzite GaN/$Al_xGa_{1-x}N$ cylindrical quantum dots

Let us now consider a single cylindrical WZ GaN QD with radius R and height L, surrounded by a large energy gap material WZ GaN / $Al_xGa_{1-x}N$, in which the origin is taken at the center of the QD and the z axis is defined to be the growth direction. Within the framework of effective-mass approximation, the Hamiltonian of the exciton can be written as

$$\hat{H}_{ex}=\hat{H}_e+\hat{H}_h+E_g-\frac{e^2}{4\pi\varepsilon_0\bar{\varepsilon}\,|\boldsymbol{r}_e-\boldsymbol{r}_h|} \tag{1}$$

where $\hat{H}_e(\hat{H}_h)$ is the electron (hole) Hamiltonian, E_g is the band gap energy of the WZ GaN material, $\boldsymbol{r}_e(\boldsymbol{r}_h)$ is the position vector of the electron (hole). e is the absolute value of the electron charge, ε_0 is the permittivity of free space, and $\bar{\varepsilon}$ is the effective mean relative dielectric constant of the embedding material between the electron and hole.

The Hamiltonian of the electron (hole) in the cylindrical coordinates reads

$$\hat{H}_j=-\frac{\hbar^2}{2m_j^*}\left[\frac{1}{\rho_j}\frac{\partial}{\partial\rho_j}\left(\rho_j\frac{\partial}{\partial\rho_j}\right)+\frac{1}{\rho_j^2}\frac{\partial^2}{\partial\varphi_j^2}+\frac{\partial^2}{\partial z_j^2}\right]+V(\rho_j)+V(z_j)\mp eFz_j \tag{2}$$

where the subscript j=e or h denotes the electron or hole. m_j^* is the electron (hole) effective mass. The sign $-(+)$ is for electron (hole). F is the BEF caused by the spontaneous and piezoelectric polarizations in the WZ GaN/$Al_xGa_{1-x}N$ QD. For infinitely thick barriers, the strength of F in the WZ GaN/$Al_xGa_{1-x}N$ QD is expressed as[20]

$$\begin{cases}F^{GaN}=\left|-\dfrac{P_{sp}^{GaN}\hat{z}+P_{pE}^{GaN}\hat{z}-P_{sp}^{Al_xGa_{1-x}N}\hat{z}}{\varepsilon_e^{GaN}\varepsilon_0}\right| \\ F^{Al_xGa_{1-x}N}\rightarrow 0\end{cases} \tag{3}$$

where P_{sp}^{GaN}, P_{pE}^{GaN} and $P_{sp}^{Al_xGa_{1-x}N}$ are the spontaneous and piezoelectric polarizations of GaN and the spontaneous polarization of GaN/$Al_xGa_{1-x}N$, respectively. ε_e^{GaN} is the electronic dielectric constant of material GaN.

In Eq. (2), $V(\rho_j)$ and $V(z_j)$ are the in-plane and z-direction confinement potential due to the band offset (Q_j) in the WZ GaN/$Al_xGa_{1-x}N$ QD, respectively. They can be given by

$$V(\rho_j)=\begin{cases}0 & (\rho_j\leqslant R)\\ Q_j[E_g(Al_xGa_{1-x}N)-E_g(GaN)] & (\rho_j>R)\end{cases} \tag{4}$$

$$V(z_j)=\begin{cases}0 & (|z_j|\leqslant\frac{L}{2})\\ Q_j[E_g(Al_xGa_{1-x}N)-E_g(GaN)] & (|z_j|>\frac{L}{2})\end{cases} \tag{5}$$

In this paper, the ratio of the conduction band to the valence band offset is assumed to be 75 ∶ 25[5,14].

The wave function of the electron (hole) confined in the WZ GaN/$Al_xGa_{1-x}N$ QD can be written as

$$\psi_j(\rho_j,\varphi_j,z_j)=f(\rho_j)h(z_j)e^{im\varphi_j} \quad m=0,\pm1,\pm2,\cdots \tag{6}$$

where m is the electron (hole) z-component angular momentum quantum number. The radial wave function $f(\rho_j)$ of the electron (hole) can be obtained by using the Bessel function J_m and the modified Bessel function K_m. Wave function $h(z_j)$ can be expressed by means of the Airy functions A_i and B_i.

In order to calculate the exciton binding energy, the trial wave function can be chosen as[21-22]

$$\Phi_{ex}(\boldsymbol{r}_e,\boldsymbol{r}_h)=\psi_e(\rho_e,\varphi_e,z_e)\psi_h(\rho_h,\varphi_h,z_h)\times e^{-\alpha\rho_{eh}^2}e^{-\beta z_{eh}^2} \quad (7)$$

where $\psi_e(\psi_h)$ is the electron (hole) wave function confined in the QD, $\rho_{eh}^2=\rho_e^2+\rho_h^2-2\rho_e\rho_h\cos(\varphi_e-\varphi_h)$, $z_{eh}^2=(z_e-z_h)^2$, α and β are variational parameters.

The ground-state energy of the exciton can be determined by

$$E_{ex}=\min_{\alpha,\beta}\frac{\langle\Phi_{ex}|\hat{H}_{ex}|\Phi_{ex}\rangle}{\langle\Phi_{ex}|\Phi_{ex}\rangle} \quad (8)$$

The exciton binding energy E_b and the optical transition energy E_{ph} can be defined as follows,

$$E_b=E_e+E_h+E_g-E_{ex} \quad (9)$$

$$E_{ph}=E_g+E_e+E_h-E_b \quad (10)$$

where $E_e(E_h)$ is the electron (hole) confinement energy in the QD.

The emission wavelength associated with the exciton can be represented as

$$\lambda=\frac{hc}{E_{ex}} \quad (11)$$

The probability of radiative transition associated with the exciton states described by the wave function (Eq. (7)) is proportional to the square of the overlap integral defined as[21]

$$M_{e-h}^2=|\int d\boldsymbol{r}_e d\boldsymbol{r}_h\Phi_{ex}(\boldsymbol{r}_e,\boldsymbol{r}_h)\delta(\boldsymbol{r}_e-\boldsymbol{r}_h)|^2 \quad (12)$$

Since the strong BEF pushes the electron and hole to opposite directions, causing "spatial separation" between the electron and hole in the QD, the in-plane distance $\bar{\rho}_{eh}$ and the distance $\bar{z}_{eh}$ in the z direction are defined as[21]

$$\bar{\rho}_{eh}^2=\frac{\langle\Phi(\boldsymbol{r}_e,\boldsymbol{r}_h)|\rho_{eh}^2|\Phi(\boldsymbol{r}_e,\boldsymbol{r}_h)\rangle}{\langle\Phi(\boldsymbol{r}_e,\boldsymbol{r}_h)|\Phi(\boldsymbol{r}_e,\boldsymbol{r}_h)\rangle} \quad (13)$$

$$\bar{z}_{eh}^2=\frac{\langle\Phi(\boldsymbol{r}_e,\boldsymbol{r}_h)|(z_e-z_h)^2|\Phi(\boldsymbol{r}_e,\boldsymbol{r}_h)\rangle}{\langle\Phi(\boldsymbol{r}_e,\boldsymbol{r}_h)|\Phi(\boldsymbol{r}_e,\boldsymbol{r}_h)\rangle} \quad (14)$$

1.2 Pressure and strain dependence of parameters

The pressure- and strain-dependent energy gaps of GaN and AlN are[18]

$$E_{g,GaN}=E_{g,GaN}(P)+2(a_{2,GaN}+b_{2,GaN})\varepsilon_{xx,GaN}+(a_{1,GaN}+b_{1,GaN})\varepsilon_{zz,GaN} \quad (15)$$

$$E_{g,AlN}=E_{g,AlN}(P)+2a_{2,AlN}\varepsilon_{xx,AlN}+a_{1,AlN}\varepsilon_{zz,AlN} \quad (16)$$

where $a_{1,i}$, $a_{2,i}$, $b_{1,i}$ and $b_{2,i}$ (i=GaN or AlN) are the deformation potentials. The dependence of the energy gap on hydrostatic pressure P is considered by the following equation is[23]

$$E_{g,i}(P)=E_{g,i}(0)+\chi_i P+\tau_i P^2 \quad (17)$$

The energy gap of ternary mixed crystal GaN/$Al_xGa_{1-x}N$ (chosen as the barriers) is[5]

$$E_{g,Al_xGa_{1-x}N}=E_{g,GaN}(1-x)+E_{g,AlN}x-1.3(\mathrm{eV})x(1-x) \quad (18)$$

Within the infinitely thick barrier approximation, the biaxial lattice-mismatch induced strain in the GaN QD are given as[24]

$$\varepsilon_{xx,GaN}=\varepsilon_{yy,GaN}=\frac{a_{AlGaN}(P)-a_{GaN}(P)}{a_{GaN}(P)} \quad (19)$$

where $a_{AlGaN}(P)$ and $a_{GaN}(P)$ represent the a-axis lattice constant of GaN/$Al_xGa_{1-x}N$ and GaN. The lattice constant as a function of hydrostatic pressure is given by[25]

$$a_i(P)=a_{0i}\left(1-\frac{P}{3B_{0i}}\right) \quad (20)$$

where superscript i=w or b donates the well or barrier materials. Bulk modulusB_{0i} in a wurtzite structure is given by elastic constants C_{11}, C_{12}, C_{13} and C_{33} as[24]

$$B_{0i}=\frac{(C_{11,i}+C_{12,i})C_{33,i}-2C_{13,i}^2}{C_{11,i}+C_{12,i}+2C_{33,i}-4C_{13,i}} \quad (21)$$

Based on the Hooke's law, the ratio of the in-plane strain component and the strain component along the c axis can be expressed by[24]

$$\frac{\varepsilon_{zz,i}}{\varepsilon_{xx,i}}=\frac{C_{11,i}+C_{12,i}-2C_{13,i}}{C_{33,i}-C_{13,i}} \quad (22)$$

The strain and hydrostatic pressure dependences of the effective masses of an electron in the z direction and the $x-y$ plane can be calculated by[26-27]

$$\frac{m_0}{m_{e,i}^{\perp,//}(P)}=1+\frac{C}{E_{g,i}} \quad (23)$$

Here C is a constant and can be determined by solving Eq. (23) at $P=0$. In general, the pressure coefficient for a heavy-hole is assumed to be zero.

The static dielectric constant ε_s is influenced by hydrostatic pressures and the biaxial strains. The tensor components of ε_s for the wurtzite structure are derived from the generalized Lyddane-Sachs-Teller relation[24]

$$\varepsilon_{s,\delta\delta}(p)=\varepsilon_{\infty,\delta\delta}(p)\left(\frac{\omega_{Lo,\delta\delta}}{\omega_{To,\delta\delta}}\right)^2 \quad (24)$$

Here, the frequencies of LO- and TO-phonons influenced by pressure and strain can be written as[24]

$$\omega_{j,\delta\delta}=\omega_{j,\delta\delta}(P)+2K_{j,xx}\varepsilon_{xx}+K_{j,zz}\varepsilon_{zz} \quad (25)$$

where $K_{j,xx}$ and $K_{j,zz}$ are the strain coefficients of phonon modes given in Ref. [24]. j represents LO- or TO-phonon. The tensor component ($\delta=z$, x) is related to the LO-and TO-phonon frequencies, respectively. Furthermore, the hydrostatic pressure dependence of $\omega_{j,\delta\delta}(P)$ can be determined by the given mode Grüneisen parameter[26-27]

$$\gamma_{j,\delta\delta}=B_0\frac{1}{\omega_{j,\delta\delta}}\frac{\partial\omega_{j,\delta\delta}(P)}{\partial P} \quad (26)$$

Considering the influence of hydrostatic pressure, the high frequency dielectric constant in Eq. (24) can be written as[26-27]

$$\frac{\partial\varepsilon_{\infty,\alpha\beta}(P)}{\partial P}=-\frac{5(\varepsilon_{\infty,\alpha\beta}-1)}{3B_0}(0.9-f_{ion}) \quad (27)$$

where $f_{\rm ion}$ is the ionicity of the material under pressure.

The effective mean relative dielectric constant in Eq. (1) is defined as

$$\bar{\varepsilon}(P)=\frac{2}{3}\varepsilon_{s,xx}(P)+\frac{1}{3}\varepsilon_{s,zz}(P) \quad (28)$$

The strain-induced piezoelectric polarizations in Eq. (3) is written as[28]

$$P_{\rm pE}^{\rm GaN}=2e_{31}(P)\varepsilon_{xx}+e_{33}(P)\varepsilon_{zz} \quad (29)$$

where e_{31} and e_{33} are the pressure-and strain-dependent piezoelectric constants of GaN satisfying[28]

$$e_{31}(P)=e_{31}(0)+\frac{4Z^*e}{\sqrt{3}a_{\rm GaN}^2(P)}\frac{{\rm d}\mu}{{\rm d}\varepsilon_{xx}} \quad (30)$$

$$e_{33}(P)=e_{33}(0)+\frac{4Z^*e}{\sqrt{3}a_{\rm GaN}^2(P)}\frac{{\rm d}\mu}{{\rm d}\varepsilon_{zz}} \quad (31)$$

where $e_{31}(0)$ and $e_{33}(0)$ are the clamped-ion terms that represent the effects of strain on the electronic structure, and the second term in Eqs. (30) and (31) is the contribution resulting from the relative displacement of the anion and cation sublattices (internal strain term). The other quantities in Eqs. (30) and (31) are the Born effective charge Z^* along the c axis, the lattice constant $a_{\rm GaN}(P)$ of GaN, and the internal parameter μ. From Ref. [24], we can obtain $Z^*=1.18$, $\frac{{\rm d}\mu}{{\rm d}\varepsilon_{zz}}=-0.208$, $\frac{{\rm d}\mu}{{\rm d}\varepsilon_{xx}}=0.262$.

The pressure-dependent radius and height of the GaN QD may be obtained from the fractional change in volume associated with the hydrostatic pressure[29]

$$\frac{\Delta V}{V_0}=-3P(S_{11}+2S_{12}) \quad (32)$$

with $V(P)=\pi R^2(P)L(P)$, $V_0=\pi R_0{}^2L_0$, $\Delta V=V(P)-V_0$, and therefore

$$R(P)=R_0[1-3P(S_{11}+2S_{12})]^{1/3} \quad (33)$$

$$L(P)=L_0[1-3P(S_{11}+2S_{12})]^{1/3} \quad (34)$$

where R_0 (L_0) is the radius (height) of QD at atmospheric pressure, and S_{11} and S_{12} are the compliance constants of GaN given by[29]

$$S_{11}=\frac{(C_{11,\rm GaN}+C_{12,\rm GaN})}{(C_{11,\rm GaN}-C_{12,\rm GaN})(C_{11,\rm GaN}+2C_{12,\rm GaN})} \quad (35)$$

$$S_{12}=-\frac{C_{12,\rm GaN}}{(C_{11,\rm GaN}-C_{12,\rm GaN})(C_{11,\rm GaN}+2C_{12,\rm GaN})} \quad (36)$$

2 Numerical results and discussion

We have calculated the exciton binding energies and emission wavelengths, and investigated the electron-hole recombination rates in strained WZ $\rm GaN/Al_{0.15}Ga_{0.85}N$ cylindrical QD with finite height potential barriers by considering hydrostatic pressure effects. For simplicity, we concentrate on the heavy-hole exciton states in the following. All material parameters used in our calculations are listed in Tables 1～3.

Table 1 Physical parameters of wurtzite GaN and AlN used in the computation

	a/nm	C_{11}/GPa	C_{12}/GPa	C_{13}/GPa	C_{33}/GPa	e_{31}/(C·m^{-2})	e_{33}/(C·m^{-2})	$P^{\rm SP}$/(C·m^{-2})
GaN	0.3189[a]	390[b]	145[b]	106[b]	398[b]	−0.49[c]	0.73[c]	−0.029[c]
AlN	0.3112[a]	398[b]	140[b]	127[b]	382[b]			−0.081[c]

[a] Reference[30], [b] Reference[31], [c] Reference[32]

Table 2 Other physical parameters of wurtzite GaN and AlN used in the computation

	E_g/meV	$m_e{}^*/m_0$	χ/(meV·GPa^{-1})	τ/(meV·GPa^{-2})	$f_{\rm ion}$	a_1/meV	a_2/meV	b_1/meV	b_2/meV
GaN	3507[a]	0.2[a]	33[b]	−0.32[c]	0.5[d]	−4090[e]	−8870[e]	−7020[e]	3650[e]
AlN	6230[a]	0.32[a]	43[b]	−0.32[c]	0.499[d]	−3390[e]	−11810[e]	−9420[e]	4020[e]

[a] Reference[30], [b] Reference[33], [c] Reference[23], [d] Reference[18], [e] Reference[24]

Table 3 Other physical parameters of wurtzite GaN and AlN used in the computation

	$\kappa_{\infty,xx}$	$\kappa_{\infty,zz}$	$\omega_{{\rm LO},xx}$/cm^{-1}	$\omega_{{\rm LO},zz}$/cm^{-1}	$\omega_{{\rm TO},xx}$/cm^{-1}	$\omega_{{\rm TO},zz}$/cm^{-1}	$\gamma_{{\rm LO},xx}$	$\gamma_{{\rm LO},zz}$	$\gamma_{{\rm TO},xx}$	$\gamma_{{\rm TO},zz}$
GaN	5.20[a]	5.39[a]	757[b]	748[b]	568[b]	541[b]	0.99[b]	0.98[b]	1.19[b]	1.21[b]
AlN	4.30[a]	4.52[a]	924[b]	898[b]	677[b]	618[b]	0.91[b]	0.82[b]	1.18[b]	1.02[b]

[a] Reference[24], [b] Reference[15]

A comparison between the theoretical and measured optical transition energies under zero hydrostatic pressure is presented in Table 4. For comparison, the results calculated by Dai *et al* without considering the strain dependence of material parameters are also listed. The good agreement between the present theoretical results and the previous experimental findings suggests that the models are suitable for investigating excitonic properties in GaN QD nanostructures. Comparing to the results calculated by Dai *et al*[13] without considering the strain dependence of material parameters, one can see that the strain dependence of material parameters isn't ignorable, especially for the small QDs with large Al content.

Table 4 Calculated and measured optical transition energies at zero hydrostatic pressure in GaN/ $Al_xGa_{1-x}N$ QDs

L/nm	R/nm	x	E_{ph}^{exper}/eV	E_{ph}^{calc}/eV Present	E_{ph}^{calc}/eV Dai	Error/(%) Present	Error/(%) Dai
3.5	5	0.15	3.581[a]	3.560	3.509[b]	0.59	2[b]
5.5	25	0.10	3.440[c]	3.443	3.414[b]	0.09	0.7[b]

[a]Reference[5], [b]Reference[13], [c]Reference[6]

In Fig. 1, the effective relative dielectric constants GaN and AlN and the mean relative distance of the electron-hole pair in the z-direction are calculated as a function of the hydrostatic pressure. Numerical results show that the effective relative dielectric constants of GaN and AlN linearly decrease with increasing hydrostatic pressure. Furthermore, Fig. 1 also shows that the distance $\bar{z}_{eh}$ in the z-direction between the electron and hole is approximately linearly reduced with the increase of hydrostatic pressure. The reason is that the volume of the QD decreases and confining effects reduce the e-h distance with increasing hydrostatic pressure.

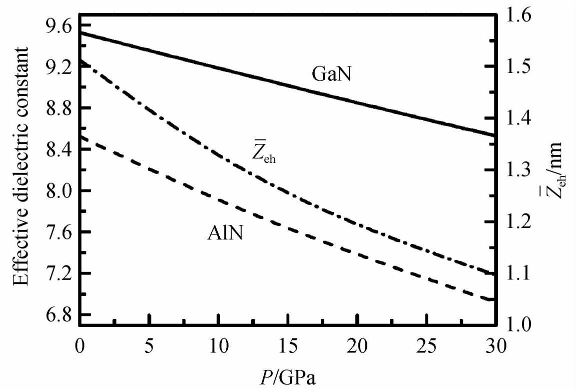

Fig. 1 The effective relative dielectric constants and the distance $\bar{z}_{eh}$ between the electron and hole as a function of the hydrostatic pressure

In Fig. 2 we present our results for the heavy-hole exciton binding energy. In Fig. 2 (a) and Fig. 2(b), we note that the exciton binding energies increase linearly with increasing the hydrostatic pressure. The pressure-related changes are mainly due to the pressure dependence of both the effective relative dielectric constant and the volume of QD. The behavior is as follows. As the hydrostatic pressure increases: 1) the effective relative dielectric constant decreases leading to an increase of the energy of the correlated e-h pair; 2) the volume of the QD decreases and the electron-hole spatial separation is reduced (see Fig. 1) leading to an increase of the exciton binding energy.

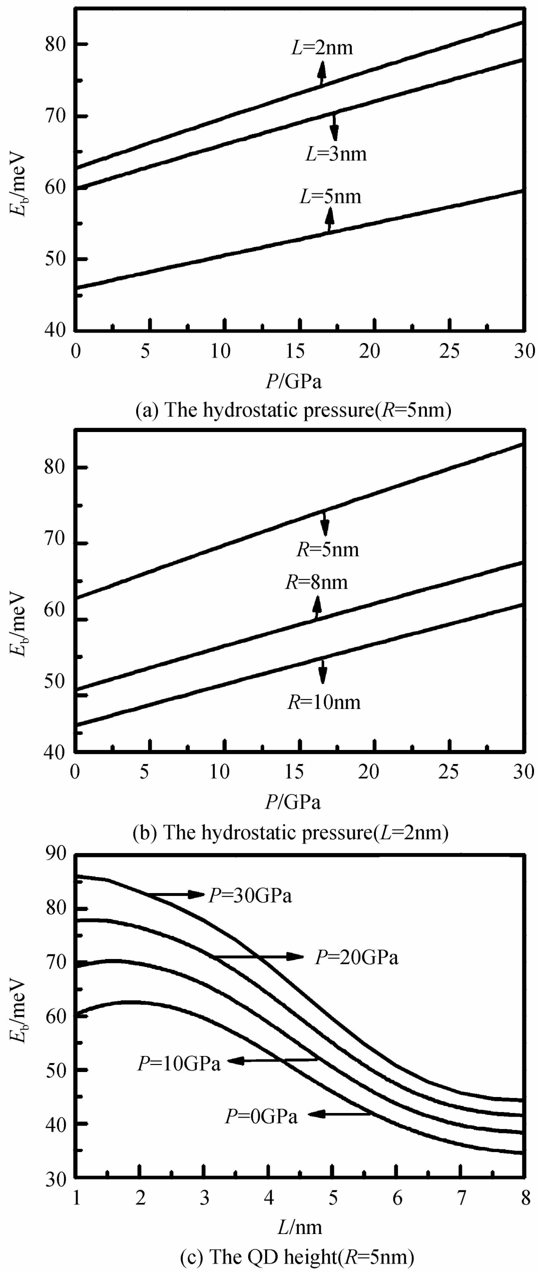

Fig. 2 Heavy-hole exciton binding energy E_b as functions of the hydrostatic pressure and the QD height

Moreover, we can find from Fig. 2(a) and Fig. 2(b) that the pressure has a remarkable influence on the exciton binding energy for the small QD. From the results in Fig. 2(c), it is clear that when the applied hydrostatic pressure is ≤ 10 GPa the binding energy grows up to a maximum and then slowly decreases with decreasing the QD height. This well-known behavior of the increase in the exciton binding energy is associated with the reduction of the electron-hole distance with decreasing the QD height. In the case the QD height is ≤2 nm the electron (hole) wave function spreads into the barrier region, the binding energy is reduced due to the decreasing coulomb interaction between the electron and the hole.

However, in the case the applied hydrostatic pressure is >10 GPa, the exciton binding energy increases monotonically as the QD height diminishes. This reason is that the binding energy is remarkably increased due to the increase of the applied hydrostatic pressure for the small QD, this induces that the point of maximum lying in about 2 nm disappears.

Fig. 3 displays the emission wavelength λ as functions of both the hydrostatic pressure and the QD height in the QD with radius $R=5$ nm. Fig. 3(a) indicates that the emission wavelength monotonically decreases if the hydrostatic pressure is increased. This result can be explained by the increase of the effective band gap of the GaN layer due to the hydrostatic pressure. In Fig. 3(a), we also observe that the emission wavelength shows a linear decrease for $P \leqslant 5$ GPa, and for larger values of the applied hydrostatic pressure, the quadratic term in the pressure [Eq. (17)] begins to be of importance, leading to a slower decrease of the emission wavelength. Furthermore, we can see from Fig. 3(b) that for a given value of the applied hydrostatic pressure the emission wavelength almost linearly increases if the height L is increased. The reason is that the strong BEF induces a redshift of the effective band gap of GaN layer. Therefore, the emission wavelength increases with increasing the QD height.

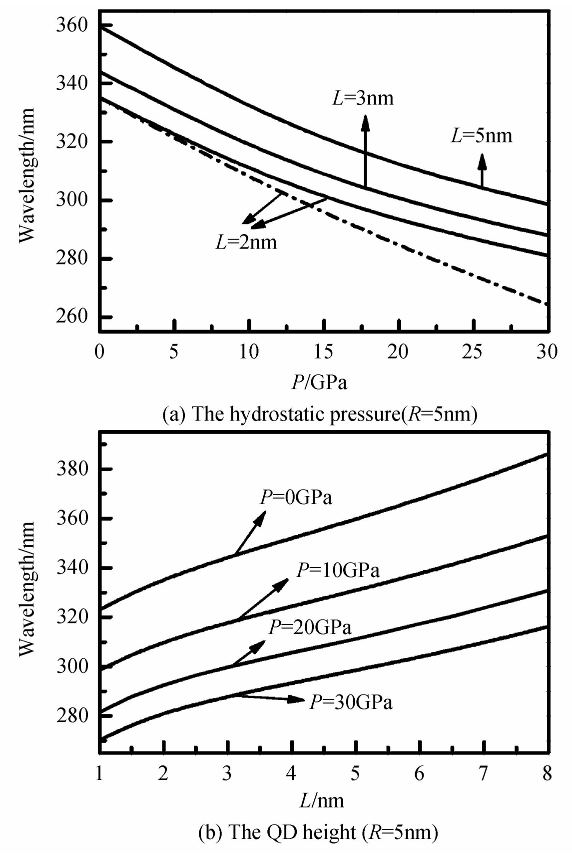

Fig. 3 The emission wavelength as functions of the hydrostatic pressure and the QD height(the dot-dashed line is for $\tau=0$ in Eq. (17))

Fig. 4 shows that the electron-hole recombination rate as functions of both the hydrostatic pressure and the QD height in the QD with radius $R=5$ nm. The electron- hole recombination rate linearly increases with increaseing hydrostatic pressure, as shown in Fig. 4(a). This is because the electron-hole spatial separation is reduced with increasing hydrostatic pressure (see Fig. 1). And the pressure has a significant influence on the electron-hole recombination rate for the small QD. In addition, we note [Fig. 4(b)] that the electron-hole recombination rate is reduced quickly if L is increased. The reason is that the electron-hole spatial separation in the z-direction is enlarged when L is increased. For a large height L ($L \geqslant 5.5$ nm), Fig. 4(b) also shows that the electron-hole recombination rate both approaches almost zero for the different values of hydrostatic pressure. Therefore, the height of GaN QDs must be less than 5.5 nm for an efficient electron-hole recombination process. This finding is extremely

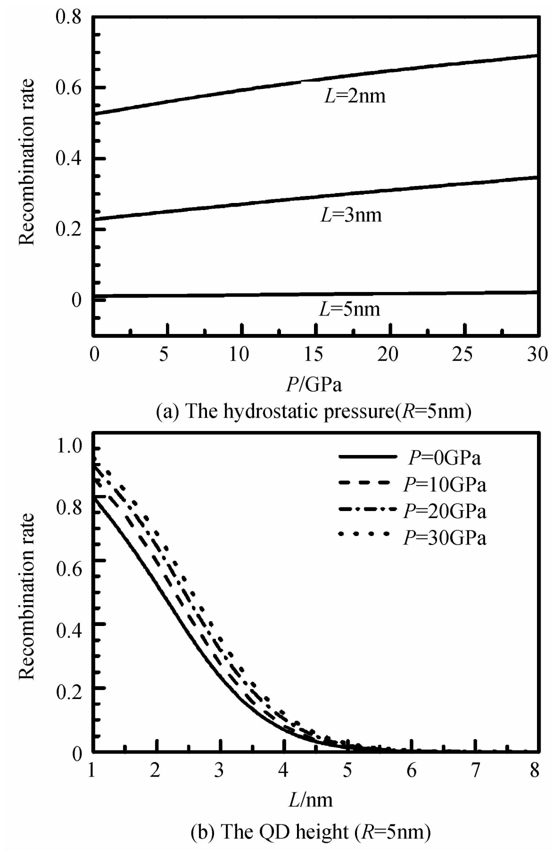

Fig. 4 Electron-hole recombination rate as functions of the hydrostatic pressure and the QD height

important for QD device applications.

3 Conclusions

In conclusion, we have investigated the effects of hydrostatic pressure on the binding energy, emission wavelength, and electron-hole recombination rate for a heavy-hole exciton in strained WZ GaN/$Al_{0.15}Ga_{0.85}N$ cylindrical QD, considering the strong built-in electric field effect and strain dependence of material parameters. Calculations are performed by a variational procedure within the effective-mass and finite potential barriers approximation. The exciton binding energy, emission wavelength, and electron-hole recombination rate sensitively depend on the QD height and hydrostatic pressure. Size effects show that as the QD height increases the exciton binding energy monotonically decreases for larger values of the hydrostatic pressure, and the emission wavelength increases, and the electron-hole recombination rate decreases. Pressure effects show that the exciton binding energy and electron-hole recombination rate both increase almost linearly, and the emission wavelength is reduced with the increase of the applied hydrostatic pressure mainly due to the pressure variation of the dielectric constant and volume of the QD. In order to achieve an effective electron-hole recombination process, the height of QDs usually should be less than 5.5 nm. Moreover, we hope that our theory can stimulate further investigations of the physics, as well as device applications of group-III nitrides. In the sense that convenient optoelectronic behavior may be achieved by properly varying either the QD size or applying hydrostatic pressure.

References

[1] WU C W, BELL A, PONCE F A, *et al*. Growth of self-assembled GaN quantum dots via the vapor - liquid - solid mechanism[J]. *Applied Physics Letters*, 2002, **81**(17): 3236-3238.

[2] KAWASAKI K, YAMAZAKI D, KINOSHITA A, *et al*. GaN quantum-dot formation by self-assembling droplet epitaxy and application to single-electron transistors[J]. *Applied Physics Letters*, 2001, **79**(14): 2243-2245.

[3] RANJAN V, ALLAN G, PRIESTER C, *et al*. Self-consistent calculations of the optical properties of GaN dots[J]. *Physical Review B*, 2003, **68**(11): 115305 (1-7).

[4] de RIINALDIS S, D' AMICO I, ROSSI F. Exciton-exciton interaction engineering in coupled GaN quantum dots[J]. *Applied Physics Letters*, 2002,**81**(22): 4236-4238.

[5] RAMVALL P, TANAKA S, NOMURA S, *et al*. Observation of confinement-dependent exciton binding energy of GaN quantum dots[J]. *Applied Physics Letters*, 1998, **73**(8): 1104-1106.

[6] TANAKA S, LEE J S, RAMVALL P, *et al*. A UV light-emitting diode incorporating GaN quantum dots[J]. *Japanese Journal of Applied Physics*, 2003, **42**(8A): L885-L887.

[7] RAMVALL P, RIBLET P, NOMURA S, *et al*. Optical properties of GaN quantum dots[J]. *Journal of Applied Physics*, 2000, **87**(8): 3883-3890.

[8] LITVINOV V I. Optical transitions and gain in group-III nitride quantum wells[J]. *Journal of Applied Physics*, 2000, **88**(10): 5814 -5819.

[9] WAN S P, XIA J B, CHANG K. Effects of piezoelectricity and spontaneous polarization on electronic and optical properties of wurtzite III - V nitride quantum wells[J]. *Journal of Applied Physics*, 2001, **90**(12): 6210-6216.

[10] FONOBEROV V A, BALANDIN A A. Excitonic properties of strained wurtzite and zinc- blende GaN/$Al_xGa_{1-x}N$ quantum dots[J]. *Journal of Applied Physics*, 2003, **94**(11): 7178-7186.

[11] FONOBEROV V A, POKATILOV E P, BALANDIN A A. Interplay of confinement, strain, and piezoelectric effects in the optical spectrum of GaN quantum dots[J]. *Journal of Nanoscience and Nanotechnology*, 2003, **3**(3): 253-256.

[12] de RINALDIS S, AMICO I D, ROSSI F. Intrinsic electric field effects on few-particle interactions in coupled GaN quantum dots[J]. *Physical Review B*, 2004, **69**(23): 235316(1-9).

[13] DAI Xian-qi, HUANG Feng-zhen, SHI Jun-jie. Exciton states in strained GaN/$A1_xGa_{1-x}N$ quantum dot[J]. *Journal of Functional Materials*, 2006, **37**(1): 130-135.

[14] WEI Shu-yi, ZHAO Xu, WU Hua-rui, *et al*. Influence of built-in electric field on luminescent properties of self-formed single GaN/$Al_xGa_{1-x}N$ quantum dots[J]. *Chinese Journal of Liquid Crystals and Displays*, 2006, **21**(2): 139-144.

[15] WAGNER J M, BECHSTEDT F. Pressure dependence of the dielectric and lattice-dynamical properties of GaN and AlN [J]. *Physical Review B*, 2000, **62**(7): 4526-4534.

[16] GOÑI A R, SIEGLE H, SYASSEN K, *et al*. Effect of pressure on optical phonon modes and transverse effective charges in GaN and AlN[J]. *Physical Review B*, 2001, **64**(3): 035205(1-6).

[17] ŁEPKOWSKI S P, TEISSEYRE H, SUSKI T, *et al*. Piezoelectric field and its influence on the pressure behavior of the light emission from GaN/AlGaN strained quantum wells [J]. *Applied Physics Letters*, 2001, **79**(10): 1483-1485.

[18] HA S H, BAN S L. Binding energies of excitons in a strained wurtzite GaN/AlGaN quantum well influenced by screening and hydrostatic pressure[J]. *Journal of Physics: Condensed Matter*, 2008, **20**(8): 085218(1-7).

[19] LIU Fu-ti, ZHANG Shu-hua, GAO Zeng-hui. The optical property of GaN under high pressure[J]. *Journal of Shandong University (Natural Science)*, 2010, **45**(1): 69-72.

[20] XIA C X, WEI S Y, ZHAO X. Built-in electric field effect on hydrogenic impurity in wurtzite GaN/AlGaN quantum dot [J]. *Applied Surface Science*, 2007, **253**: 5345-5348.

[21] SHI J J, GAN Z Z. Effects of piezoelectricity and spontaneous polarization on localized excitons in self-formed InGaN quantum dots[J]. *Journal of Applied Physics*, 2003, **94**(1): 407-415.

[22] SZAFRAN B, BEDNAREK S, ADAMOWSKI J. Parity symmetry and energy spectrum of excitons in coupled self-assembled quantum dots[J]. *Physical Review B*, 2001, **64**(12): 125301(1-10).

[23] CHRISTENSEN N E, GORCZYCA I. Optical and structural

properties of III-V nitrides under pressure[J]. *Physical Review B*, 1994, **50**(7): 4397-4415.

[24] WAGNER M, BECHSTEDT F. Properties of strained wurtzite GaN and AlN: *Ab* initio studies[J]. *Physical Review B*, 2002, **66**(11): 115202(1-20).

[25] PERLIN P, MATTOS L, SHAPIRO N A, *et al*. Reduction of the energy gap pressure coefficient of GaN due to the constraining presence of the sapphire substrate[J]. *Journal of Applied Physics*, 1999, **85**(4): 2385-2389.

[26] XIA C X, ZENG Z P, WEI S Y. Effects of applied electric field and hydrostatic pressure on donor impurity states in cylindrical GaN/AlN quantum dot[J]. *Journal of Applied Physics*, 2010, **107**: 014305(1-5).

[27] ZHANG Ming, BAN Shi-liang. Stark effect of donor impurity states in strained heterojunctions under pressure[J]. *Acta Physica Sinica*, 2008, **57**(7): 4459-4465.

[28] VASCHENKO G, PATEL D, MENONI C S, *et al*. Significant strain dependence of piezoelectric constants in $In_xGa_{1-x}N$/GaN quantum wells[J]. *Physical Review B*, 2001, **64**(24): 241308(1-10).

[29] RAIGOZA N, DUQUE CA, PORRAS-MONTENEGRO N, *et al*. Correlated electron hole transition energies in quantum-well wires: Effects of hydrostatic pressure[J]. *Physica B*, 2006, **371**(1): 153-157.

[30] VURGAFTMAN I, MEYER J R, RAM-MOHAN L R. Band parameters for III-V compound semiconductors and their alloys[J]. *Journal of Applied Physics*, 2001, **89**(11): 5815-5873.

[31] PARK S H, CHUANG S L. Comparison of zinc-blende and wurtzite GaN semiconductors with spontaneous polarization and piezoelectric field effects[J]. *Journal of Applied Physics*, 2000, **87**(1): 353-364.

[32] BERNARDINI F, FIORENTINI V, VANDERBILT D. Spontaneous polarization and piezoelectric constants of III-V nitrides[J]. *Physical Review B*, 1997, **56**(16): R10024-R10027.

[33] WEI S H, ZUNGER A. Predicted band-gap pressure coefficient of all diamond and zinc-blende semiconductors: chemical trends[J]. *Physical Review B*, 1999, **60**(8): 5404-5411.

应变纤锌矿 GaN/$A1_{0.15}Ga_{0.85}$N 柱形量子点的光学性质：流体静压力效应

郑冬梅，王宗篪

（三明学院 物理与机电工程学院，福建 三明 365004）

摘　要：在有效质量近似下，考虑强的内建电场和应变对材料参量的影响，变分研究了流体静压力对有限高势垒应变纤锌矿 GaN/$Al_{0.15}Ga_{0.85}$N 柱形量子点中重空穴激子的结合能、发光波长和电子空穴复合率的影响. 数值结果表明，激子结合能和电子空穴复合率随流体静压力的增大而近线性增大，发光波长随流体静压力的增大而单调减小. 在量子点尺寸较小的情况下，流体静压力对激子结合能和电子空穴复合率的影响更明显. 由于应变效应，为了获得有效的电子-空穴复合过程，GaN 量子点的高度必须小于 5.5 nm.

关键词：量子点；激子；流体静压力；应变